

Triplet np Final State Interactions at Large Momentum Transfers

Alain Boudard¹

Service de Physique Nucléaire, CEA Saclay, F-91191 Gif-sur-Yvette, France

Göran Fäldt²

Division of Nuclear Physics, Uppsala University, Box 535, S-751 21 Uppsala, Sweden

Colin Wilkin³

University College London, London, WC1E 6BT, UK

Abstract

Using the simple relation between the np scattering and bound state wave functions, the spin-triplet contributions to the $pp \rightarrow \pi^+(pn)$ and backward $dp \rightarrow p(pn)$ reactions are estimated for low np excitation energies. The good agreement with the pion production data at 400 and 450 MeV over a range of angles shows that spin-singlet final states cannot be more than of the order of 10%. On the other hand it is seen that the spin-singlet states must provide about 30% of the strength in pion production at 1 GeV as well as deuteron-proton backward scattering at 1.6 GeV.

¹Electronic address boudard@phnx7.saclay.cea.fr

²Electronic address faldt@tsl.uu.se

³Electronic address cw@hep.ucl.ac.uk

It is well known that when a scattering wave function is extrapolated to a bound state pole then the result is proportional to the bound state wave function. Less appreciated is the fact that the constant of proportionality is *independent* of the form of the potential [1, 2]. Thus for single-channel S-wave neutron-proton scattering,

$$\lim_{k \rightarrow i\alpha_t} \left\{ -\sqrt{\frac{\alpha_t(k^2 + \alpha_t^2)}{2\pi}} e^{i\delta} \psi_k^{t(-)}(r) \right\} = \psi_d(r). \quad (1)$$

Here $\alpha_t = \sqrt{m\epsilon} = 0.232 \text{ fm}^{-1}$, where m is the average nucleon mass, ϵ the deuteron binding energy, and δ the uncoupled S-wave triplet phase shift at relative momentum \vec{k} . Though this relation is only true at the deuteron pole, nevertheless for c.m. energies below about 40 MeV and internucleon distances r less than about 1.5 fm the $^3\text{S}_1$ solution to the Paris neutron-proton potential [3] empirically behaves like

$$|\psi_k^{t(-)}(r)|^2 \approx \frac{2\pi}{\alpha_t(k^2 + \alpha_t^2)} |\psi_d(r)|^2 \quad (2)$$

to an accuracy of typically 5% [2]. Thus for large momentum transfer reactions such as π [2] or η [1] production, which are sensitive to the values of the wave functions at short distances, one can get a simple estimate of the amplitude for the production of a particle c , with a neutron-proton pair in the final state in terms of the amplitude for deuteron (d) production, *viz.*

$$M(ab \rightarrow c\{np\}_k) \approx -\sqrt{\frac{2\pi m}{\alpha_t(k^2 + \alpha_t^2)}} e^{-i\delta} M(ab \rightarrow cd). \quad (3)$$

Though there is no bound state amplitude to set the scale, the momentum dependence of the S-wave Paris singlet wave function is given by a similar $\sqrt{k^2 + \alpha_s^2}$ factor to that of eq.(1), but with a different pole parameter $\alpha_s = -0.104 \text{ fm}^{-1}$ [2, 3]. This factor in turn determines the energy variation of the production of np

singlet final states. Such a simple model for triplet and singlet production gives a good description of the total cross sections for $np \rightarrow np\eta$ [1] and $pp \rightarrow pn\pi^+$ and $pd \rightarrow pd\pi^0$ [2] near threshold. It is the aim of the present work to show that the model is equally successful at higher energies providing the neutron-proton system is constrained to be at low excitation energy.

Choosing the same normalisation for bosons and fermions, the c.m. differential cross section for the production of an N-body final state is

$$d\sigma = (2\pi)^4 \frac{1}{4p_i\sqrt{s}} \delta^{(4)}(\tilde{p}_f - \tilde{p}_i) |M|^2 \prod_{j=1}^N \frac{d^3p_j}{(2\pi)^3 2E_j}. \quad (4)$$

Here \vec{p}_j and E_j are the momentum and energy of the final-state particle j and \vec{p}_i the incident momentum corresponding to a total c.m. energy \sqrt{s} , whereas \tilde{p}_i and \tilde{p}_f are the total initial and final four-momentum vectors.

By introducing the ansatz of eq.(3) into the phase space and making kinematic approximations which are very good for high beam energies and low excitation energies $Q = k^2/m$ in the final np system, the spin-triplet contribution to the three-body cross section is predicted to be

$$\frac{d^2\sigma}{d\Omega_c dx}(ab \rightarrow c\{np\}) = \frac{p(x)}{p(-1)} \frac{\sqrt{x}}{2\pi(1+x)} \frac{d\sigma}{d\Omega_c}(ab \rightarrow cd). \quad (5)$$

The dependence on the energy of particle c is mainly through the explicit function of x , where

$$x = \frac{Q}{\epsilon} = \frac{k^2}{\alpha_t^2}. \quad (6)$$

$p(x)$ is the c.m. momentum of particle c in the $c\{np\}$ system, becoming equal to that in the cd system when $x = -1$. The ratio $p(x)/p(-1)$ is independent of angle and depends weakly upon x and the incident beam energy.

The most extensive measurement of the $pp \rightarrow \pi^+pn$ cross section and analysing power was carried out several years ago at TRIUMF at 400 and 450 MeV at several fixed laboratory angles [4]. Unfortunately the data are no longer available in numerical form but it is possible to read values from the published work [4] and the original hand-drawn graphs [5] to a fair accuracy. It is known over a wide energy domain from threshold up to the Δ -region that the final spin-triplet states dominate the reaction [6] and indeed it was noted that the $pp \rightarrow \pi^+pn$ analysing powers follow closely those of $pp \rightarrow \pi^+d$ at the same c.m. pion production angle [4].

On the basis of eq.(5), the triplet contribution to the cross section ratio is

$$R = 2\pi\epsilon \frac{d^2\sigma}{d\Omega_c dQ}(ab \rightarrow c\{np\}) \bigg/ \frac{d\sigma}{d\Omega_c}(ab \rightarrow cd) = \frac{p(x)}{p(-1)} \frac{\sqrt{x}}{1+x}. \quad (7)$$

A crucial point is that the same $pp \rightarrow \pi^+d$ cross sections employed in the normalisation in the original data analysis has to be used when constructing the experimental value of the ratio. This information is indeed available [5].

In fig. 1 all the data at the two energies and eleven laboratory angles are plotted against Q and their mutual consistency and the agreement with the predictions of eq.(7) at small Q is impressive. The immediate conclusions that one can infer from this comparison are:

1. Since any contributions from spin-singlet and P-wave final states to the semi-inclusive cross sections are incoherent and non-negative, the experimental points should not lie below the theoretical curves. Violations of this bound occur at large laboratory angles where, due to kinematic effects, the experimental resolution is poorer. The isolation of unbound

final neutron-proton states from the deuteron peak, which is not shown but which is used to normalise the cross section, becomes more difficult under such conditions.

2. Taking into account that eq.(2) may be in error by of the order of 5%, the possible amount of spin-singlet final np states must be generally less than about 10% of the spin-triplet.
3. There is evidence from the more reliable small angle points that, above an excitation energy of 10 MeV, the curves represent a smaller fraction of the data, as would be expected from the neglect of P and higher waves in the np system.
4. It has been pointed out [4] that the angular distribution of the proton analysing power follows closely that of $pp \rightarrow \pi^+d$ at low excitation energy. Apart from the larger angle points, the agreement with eq.(7) is good over a range of laboratory angles, and so this provides evidence for a similar behaviour for the differential cross section. However the resolution problem must be clarified to make this more quantitative. Fortunately the approach will soon be tested in far greater detail through the new high accuracy $pp \rightarrow \pi^+pn$ TRIUMF data currently being analysed [5].

Turning now to a second application of the technique, the momentum transfer in elastic deuteron-proton scattering in the backward direction increases very fast with beam energy. For deuteron laboratory kinetic energies below $T_d \approx 200$ MeV the process is dominated by one-neutron-exchange and the cross section then depends on the deuteron wave function at high Fermi momenta. On the other

hand, for $T_d > 800$ MeV the process is expected to be driven by pionic degrees of freedom and virtual Δ -excitation [7]. The gap region between these two models is less well understood.

The $\vec{d}p \rightarrow pd$ cross section and deuteron tensor analysing power T_{20} have been measured at 180° for $300 \leq T_d \leq 2300$ MeV and data are also available on the corresponding three-body reaction $\vec{d}p \rightarrow p(pn)$ at 400 and 1600 MeV [8]. At 1600 MeV the momentum transfer is so large that, just as for pion production, the reaction should be dominated by short-range physics. Since the energy resolution in the data is not as good as for the pion production experiment previously discussed, smearing of the predictions for the final deuteron and proton-neutron pairs over the experimental resolution function is required. Using eq.(5), the summed c.m. cross section can be written as

$$d\sigma(dp \rightarrow p\{pn\}) = \frac{p(x)}{p(-1)} \left\{ \delta(1+x) + \frac{1}{2\pi} \frac{\sqrt{x}}{1+x} \Theta(x) \right\} \frac{d\sigma}{d\Omega_p}(dp \rightarrow pd) d\Omega_p dx, \quad (8)$$

where the delta-function reflects the two-body pd final state and the term involving the theta-function the three-body triplet $p(pn)$.

Convoluting this distribution with an experimental resolution function in Q , taken to be Gaussian with $\sigma = 2.35$ MeV, leads to the spin-triplet prediction shown in fig. 2a for $T_d = 1600$ MeV. It must be stressed that it is the area of the elastic deuteron peak which fixes the normalisation of the triplet break-up contribution through eq.(8).

Unlike the low energy pion production data shown in fig. 1, our estimate leaves some space for final np singlet states. The shape of such a cross section is dominated by a similar $\sqrt{x}/(x + \alpha_s^2/\alpha_t^2)$ form but, because of the smaller value

of α_s , it is more peaked in the near-threshold region. Tolerable agreement with the data is achieved with a singlet final-state cross section about 0.4 ± 0.05 of the triplet at large Q , which is essentially consistent with a purely statistical population.

In contrast, at $T_d = 400$ MeV it is not possible to get a good fit to the data shown in fig. 2b even after including singlet np final states. The enhancement at small Q is incompatible with the data at larger values since np P-waves can only increase the cross section there. This breakdown of the model is not unexpected since at 400 MeV the one-neutron-exchange term is still the largest contribution and the short-range limit employed here is of limited value.

The difference in behaviour at the two deuteron beam energies is also seen in the deuteron tensor analysing power T_{20} . Values of this quantity were measured for the sum of the first six bins in np excitation energy as well as for elastic proton-deuteron scattering [8]. In the 1600 MeV region the difference ΔT_{20} between these two seems to be energy independent and consistent with zero. On the other hand both the elastic T_{20} and ΔT_{20} vary fast with energy in the 300 – 600 MeV region, indicating a dependence on the details of the deuteron wave function. It is clearly not the high momentum transfer domain where our approach can be used in a naive way.

The most plausible model for large angle elastic pd scattering at high energies involves the virtual production and absorption of pions [7] and the striking difference between the singlet/triplet ratio determined from pion production at 400/450 MeV and the $dp \rightarrow p(pn)$ reaction at an equivalent proton beam energy of 800 MeV could bring this into question. There is however evidence from pion

absorption on ^3He that above the Δ resonance the singlet/triplet ratio is much larger than at lower energies [6]. This is backed up by the $pp \rightarrow \pi^+pn$ data taken at 1 GeV [9] and shown in fig. 3. The absolute resolution is here a little poorer than for the 1.6 GeV $dp \rightarrow p(pn)$ experiment [8] but, when the latter data are degraded slightly by including small admixtures from neighbouring bins, the shapes of the two data sets are indistinguishable. Kinematic differences due to the variation of the pion/proton momentum with Q are negligible at such high energies. Also shown are the fitted curves of fig. 2a with the slightly increased smearing width ($\sigma = 2.60$ MeV). Pion production at 1 GeV is therefore also consistent with a singlet/triplet ratio of around 0.4 ± 0.05 .

This steady increase of the singlet/triplet ratio with beam energy at the Δ -resonance and above is confirmed in the analysis of $p(p, \pi^+)X$ results at 592 MeV and $\theta = 0^\circ$ [10]. A good fit to this data is achieved with a ratio of 0.25 ± 0.05 .

We have shown that a plausible description can be given for high momentum transfer reactions leading to unbound np scattering states at low excitation energy Q in terms of the corresponding cross section for producing a deuteron. In the limit that the transition operator is of short range our evaluation is weakly model-dependent. Our principal conclusions are that any spin-singlet final states in $pp \rightarrow \pi^+pn$ at 400 and 450 MeV must be 10% or less of the triplet, though this steadily increases to 20% and 40% at 600 and 1000 MeV respectively. This final figure, which is essentially consistent with a statistical spin factor of 3:1, also reproduces well the 1600 MeV $\vec{dp} \rightarrow ppn$ data, giving some support to the idea that this reaction is driven by virtual pion production. To go further would require the introduction of an explicit reaction model as well as a fuller evaluation

of the final neutron-proton wave function including the deuteron D-state. Our calculation has demonstrated that such a refined model should give reasonable answers. A systematic experimental study of the $pp \rightarrow \pi^+ X$ reaction in the forward direction as a function of energy should show clearly the evolution of the singlet/triplet ratio and the importance of non- Δ contributions to the reaction. The value of such experiments would be enhanced if they could be carried out with polarised beam and target since, by angular momentum conservation, in the forward direction an initial longitudinal spin-spin correlation is propagated to the final neutron-proton system.

Considerable assistance in using the data of ref.[4] was given by W.R. Falk and this made our work much easier. The values of the nucleon-nucleon S-wave singlet and triplet scattering state wave functions were kindly furnished by B. Loiseau and we have benefited greatly from his advice in their interpretation. Valuable discussions with V. Koptev are also gratefully acknowledged. This work has been made possible by the continued financial support of the Swedish Royal Academy of Science and one of the authors (CW) would like to thank them, the The Svedberg Laboratory and the Kernforschungszentrum Jülich for their generous hospitality.

References

- [1] G. Fäldt and C. Wilkin, Nucl.Phys. **A604** (1996) 441.
- [2] G. Fäldt and C. Wilkin, Phys.Lett. **B382** (1996) 209.
- [3] M. Lacombe *et al.*, Phys.Rev. **C21** (1980) 861; M. Lacombe *et al.*, Phys.Lett. B101 (1981) 139; B. Loiseau, private communication (1995).
- [4] W.R. Falk, E.G. Auld, G. Giles, G. Jones, G.J. Lolos, W. Ziegler, and P.L. Walden, Phys.Rev. **C32** (1985) 1972.
- [5] W.R. Falk, private communication (1996).
- [6] The experimental situation is well summarised in H. Hahn *et al.*, Phys.Rev. **53** (1996) 1074.
- [7] N.S. Craigie and C. Wilkin, Nucl.Phys. **B14** (1969) 477.
- [8] A. Boudard, PhD thesis, Université de Paris-sud (Orsay) 1983 (unpublished); J. Arvieux *et al.*, Phys.Rev.Lett. **50** (1983) 19.
- [9] V.V. Abaev *et al.*, Leningrad preprint LNPI-80-569 (unpublished), but see also V.V. Abaev *et al.*, J.Phys. **G14** (1988) 903.
- [10] K. Gabathuler *et al.*, Nucl.Phys. **B40** (1972) 32.

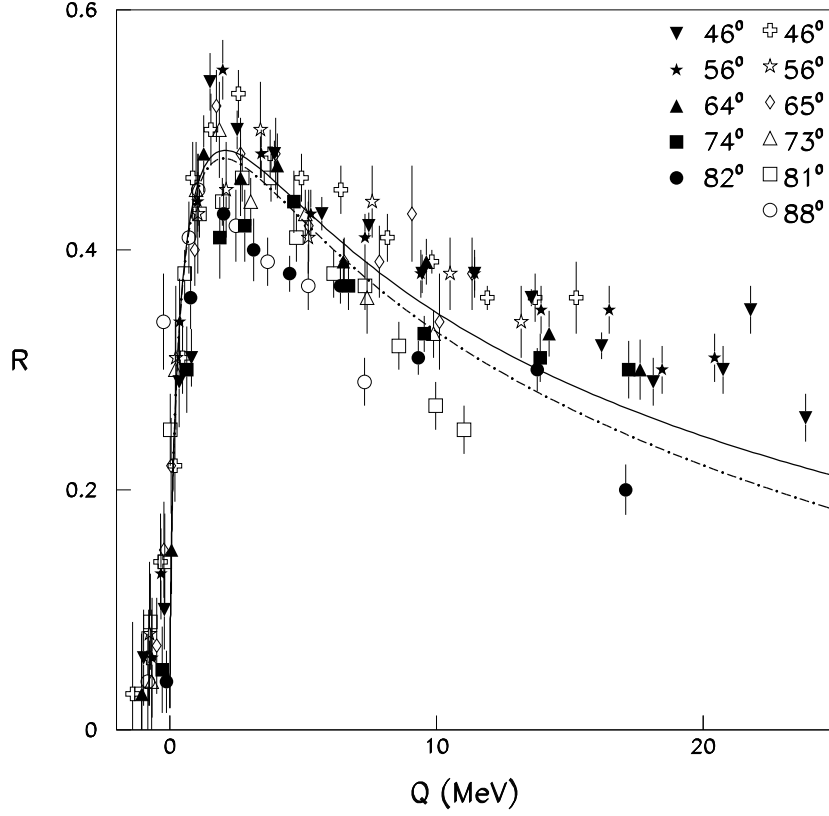


Figure 1: The ratio R of the c.m. differential cross section for $pp \rightarrow \pi^+pn$ divided by that for $pp \rightarrow \pi^+d$ at the same pion c.m. angle, as defined by eq.(7). The TRIUMF experimental data [4] were taken at 400 MeV (open symbols) and 450 MeV (closed symbols) at a total of 11 laboratory angles. The predictions of eq.(7) at these two energies are shown as the broken and solid line respectively, the only difference between them being due to the change in the variation of the momentum factor.

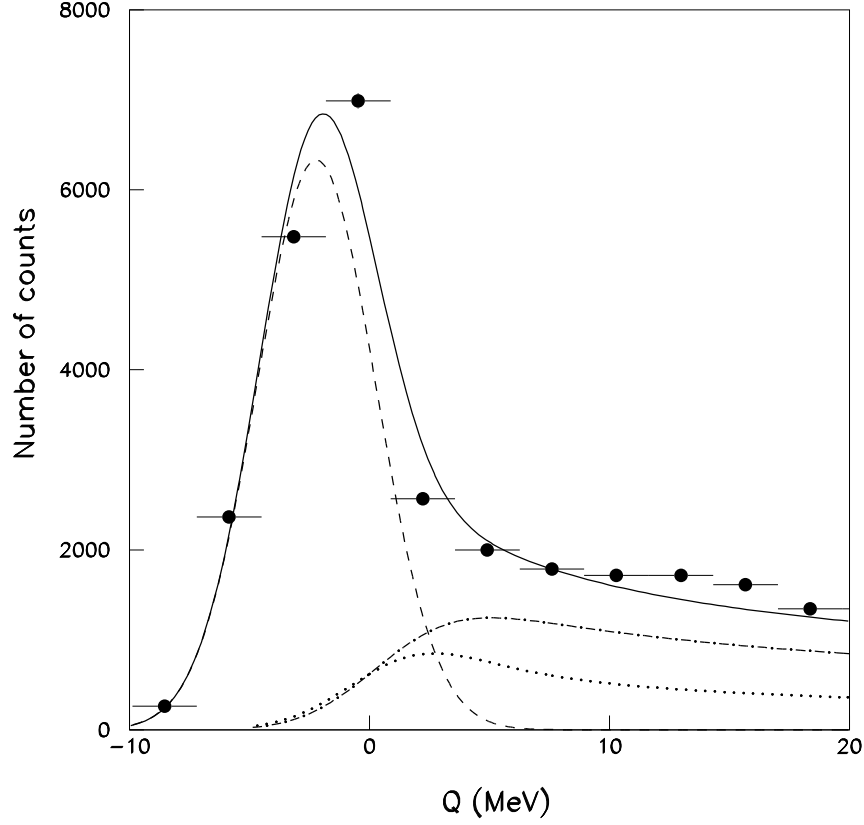


Figure 2a: Laboratory differential cross section for the $p(\vec{d}, p)pn$ reaction in the backward c.m. direction at $T_d = 1600$ MeV as a function of the excitation energy Q in the unobserved final np system [8]. The binning is such that 1 channel corresponds to 2.69 MeV. The form of eq.(8) was smeared over a Gaussian resolution function with $\sigma = 2.35$ MeV and a binning correction applied before being compared to the data. The broken line is the fitted deuteron elastic peak and the dot-dashed the resulting prediction for the triplet final np state. The amount of spin-singlet contribution required to give the overall fit (solid line) is shown as a dotted line.

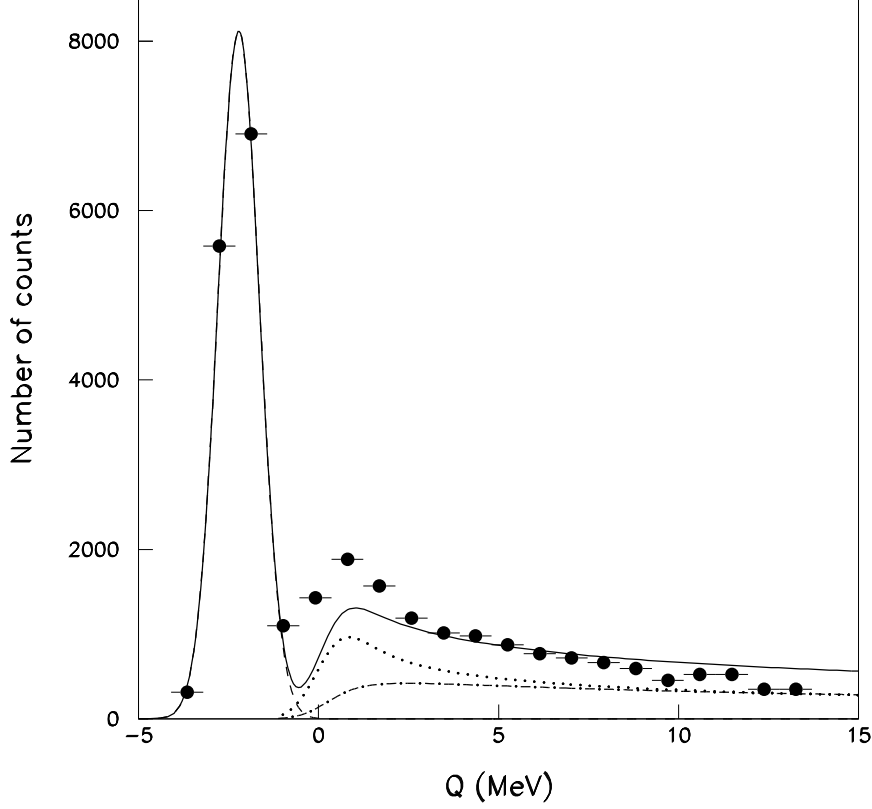


Figure 2b: Laboratory differential cross section for the $p(\vec{d}, p)pn$ reaction in the backward c.m. direction at $T_d = 400$ MeV as a function of the excitation energy Q in the unobserved final np system [8]. The binning is such that 1 channel corresponds to 0.89 MeV. The form of eq.(8) was smeared over a Gaussian resolution function with $\sigma = 0.52$ MeV and a binning correction applied before being compared to the data. The broken line is the fitted deuteron elastic peak and the dot-dashed the resulting prediction for the triplet final np state. No satisfactory overall fit to both the low and high excitation energy data (solid line) can here be achieved by adjusting the proportion of spin-singlet final states (dotted line).

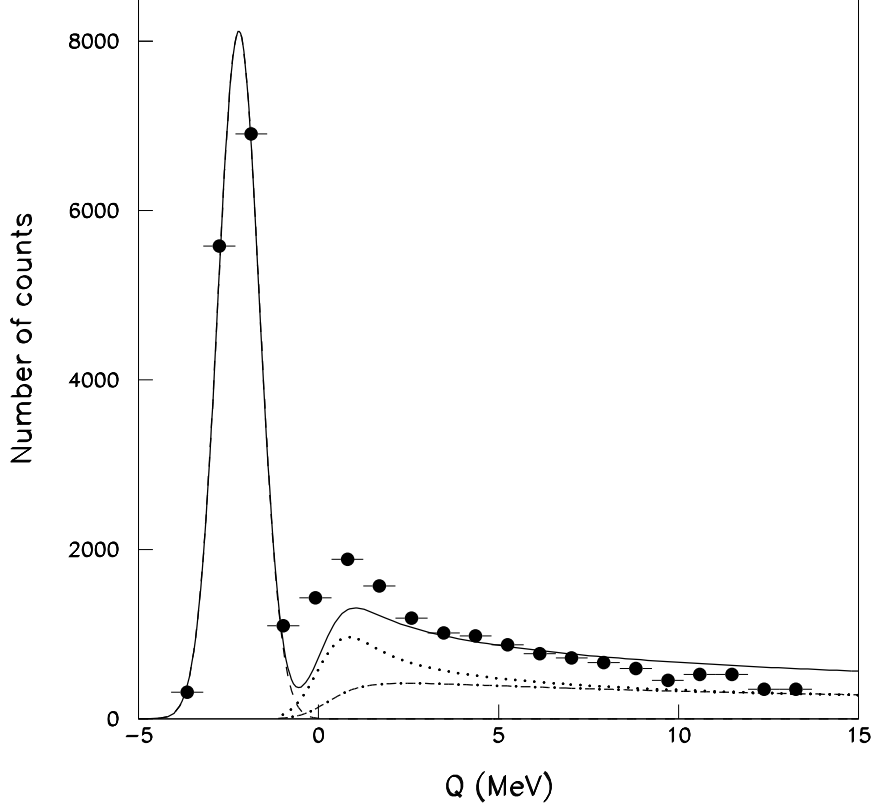


Figure 3: Laboratory differential cross section in arbitrary units for the $p(p, \pi^+)X$ reaction at $\theta = 0^\circ$ and $T_p = 1.0$ GeV (stars) as a function of the excitation energy Q in the unobserved final np system [9]. These are compared with the 1.6 GeV $p(d, p)X$ data of ref.[8] (circles) whose energy resolution has been degraded slightly by replacing the cross section $\sigma(n)$ in the n 'th bin by $0.15\sigma(n+1) + 0.7\sigma(n) + 0.15\sigma(n-1)$. The fitted curves are identical to those in fig. 2a but with a smearing parameter of $\sigma = 2.60$ MeV.

